

DOI: 10.13208/j.electrochem.121112

Cite this: *J. Electrochem.* 2014, 20(1): 17-21

Artical ID:1006-3471(2014)01-0017-05

Http://electrochem.xmu.edu.cn

# 由苯胺二聚体电化学制备聚苯胺的 形貌可控性初探

左 阳, 时 康\*

(厦门大学化学化工学院, 福建 厦门 361005)

**摘要:** 以苯胺二聚体(N-phenyl-p-phenylenediamine)为起始单体, 在  $1\text{ mol}\cdot\text{L}^{-1}$  高氯酸水-乙腈混合液中, 玻碳电极表面电化学制备聚苯胺. 实验结果表明, 苯胺二聚体单体的聚合电位比苯胺单体的低约  $0.2\text{ V}$ , 并且其聚合物具有更高的形貌可控性. 苯胺二聚体单体浓度分别为  $1, 5$  和  $10\text{ mmol}\cdot\text{L}^{-1}$  时, 采用分步恒电流法可分别制备出形貌均一的聚苯胺纳米粒子(粒径  $30\text{ nm}$ )、超长的纳米线( $> 5\text{ }\mu\text{m}$  直径  $50\text{ nm}$ )和大面积纳米片( $4\text{ }\mu\text{m} \times 2\text{ }\mu\text{m} \times 30\text{ nm}$ ).

**关键词:**  $\pi$  共轭有机导电聚合物; 聚苯胺; 单体; 电化学聚合; 均一形貌

**中图分类号:** TQ315.3

**文献标识码:** A

聚苯胺属典型的有机共轭导电聚合物有可调控的导电性、电致变色性、离子嵌入/嵌出等物化特性, 在能源、电子、分析传感和金属防腐等众多领域有着广泛的应用<sup>[1-5]</sup>. 近年研究发现聚苯胺形貌与其物化性质密切相关, 例如聚苯胺纳米管作为导电基体可与葡萄糖氧化酶直接传导电子, 而其它形貌的聚苯胺基体则无此特性, 但其中原因尚未探明<sup>[6]</sup>. 因此, 均一形貌的聚苯胺的可控制备一直是研究的热点<sup>[7-17]</sup>.

聚苯胺形貌从本质上来讲取决于其聚合反应过程机理. 大量的聚合机理研究结果业已证明, 苯胺的电化学聚合过程并不是由每一苯胺单体逐一累加形成聚合物, 而首先由苯胺单体形成二聚体, 进而形成多种低聚体, 再由低聚体间进一步聚合, 生成高分子量的聚苯胺<sup>[5, 18-25]</sup>. 因此, 以苯胺的二聚体或寡聚体为聚合反应的起始单体应是一条制得形貌均一聚苯胺的有效途径<sup>[5, 11]</sup>. 然而, 采用电化学聚合苯胺二聚体或寡聚体的研究尚未见文献报道. 早先的实验表明, 苯胺单体浓度和电化学制备方法对聚苯胺形貌的有序性和均一性至关重要, 采用高浓度苯胺单体和电化学恒电流聚合方法, 尤其分步电流法均可制成有序的聚苯胺纳米线阵列<sup>[15-16]</sup>. 本文

以苯胺二聚体(N-phenyl-p-phenylenediamine, NPD)为起始单体, 电化学恒电流聚合方法制备聚苯胺, 考察单体浓度、电流密度等因素对聚合物形貌的影响及规律.

## 1 实 验

乙腈( $\text{CH}_3\text{CN}$ ), 高氯酸( $\text{HClO}_4$ ), 苯胺(Aniline, ANI), N-苯基对苯二胺(N-phenyl-p-phenylenediamine, NPD, Sigma-Aldrich 公司), 所有试剂均为分析纯, 苯胺(减压蒸馏提纯), N-苯基对苯二胺(重结晶提纯). 所有溶液采用超纯水( $18.2\text{ M}\Omega\cdot\text{cm}$ )配制.

三电极体系, 由玻璃碳圆盘工作电极(直径  $4\text{ mm}$ , 润湿金相砂纸磨光, 而后麂皮反复打磨, 依次用  $1:1\text{ HNO}_3$ 、丙酮、去离子水超声清洗电极表面)、铂片对电极和饱和甘汞参比电极(SCE, 文中所给电位均相对此电极而言)组成. 使用 CHI660C 电化学工作站(上海辰华)电化学聚合.

恒电流: 对 NPD 或 ANI 分别以  $16\text{ }\mu\text{A}$  或  $10\text{ }\mu\text{A}$  恒电流聚合  $270\text{ s}$ .

分步恒电流: 对 NPD 先  $16\text{ }\mu\text{A}$  恒电流聚合  $45\text{ s}$ , 而后电流降至  $8\text{ }\mu\text{A}$  聚合  $270\text{ s}$ , 最后以  $4\text{ }\mu\text{A}$

聚合 270 s; 对 ANI 先以  $10\ \mu\text{A}$  恒电流聚合 45 s, 而后电流降至  $5\ \mu\text{A}$  聚合 270 s, 最后以  $2.5\ \mu\text{A}$  聚合 270 s.

使用扫描电子显微镜 (Scan Electron Microscopy, SEM, S-4800 型, 日本日立公司) 观察聚苯胺形貌.

## 2 结果与讨论

### 2.1 N-苯基对苯二胺的电化学氧化还原和聚合特性

图 1A 是玻碳电极在  $0.01\ \text{mol}\cdot\text{L}^{-1}$  NPD +  $1\ \text{mol}\cdot\text{L}^{-1}$   $\text{HClO}_4$  溶液 (20% 乙腈, by volume) 中首周期循环的 CV 曲线. 从图 1 可见, 在正向扫描过程中, NPD 单体约从  $0.4\ \text{V}$  开始发生氧化, 一个高氧化峰随之出现于  $0.53\ \text{V}$ ; 当电位高于  $0.75\ \text{V}$ , 氧化电流再次增加, 并且在  $0.75\ \text{V} \sim 0.80\ \text{V}$  区间, 负向回扫电流高于正向扫描电流, 这一现象源于低聚物对单体的氧化还原催化作用<sup>[24]</sup>, 说明聚合业已发生; 两个较明显的还原峰分别呈现于  $0.65\ \text{V}$  和

$0.50\ \text{V}$ , 并可在  $0.35\ \text{V}$  附近观测到一个宽的还原肩峰. 随周期循环次数增加 (图 1A'), 分别在  $0.25\ \text{V}$  和  $0.65\ \text{V}$  观测到两个新氧化峰, 而高于  $0.75\ \text{V}$  的氧化电流不再增加; 位于  $0\ \text{V} \sim 0.8\ \text{V}$  区间内氧化还原峰均逐渐增高, 说明聚苯胺在电极表面不断生成并沉积.

作为对比, 图 1B 给出了玻碳电极在  $0.01\ \text{mol}\cdot\text{L}^{-1}$  ANI +  $1\ \text{mol}\cdot\text{L}^{-1}$   $\text{HClO}_4$  溶液 (20% 乙腈, by volume) 中首周期循环的 CV 曲线. ANI 单体自  $0.3\ \text{V}$  开始被氧化, 随后在  $0.5\ \text{V}$  形成一个极宽的峰; 当电位高于  $0.7\ \text{V}$ , 氧化电流急剧增加, 并且负向回扫电流高于正向扫描电流; 另有两个还原峰分别出现在  $0.41\ \text{V}$  和  $0.05\ \text{V}$ . 随着周期循环继续进行 (图 1B'), 分别在  $0.18\ \text{V}$  和  $0.70\ \text{V}$  观测到两个逐渐增高的新氧化峰, 说明聚苯胺在电极表面的沉积逐渐增加.

从图 1 可见, NPD 单体及其聚合物的氧化还原行为与 ANI 单体及其聚合物的不同, 说明不仅 NPD 电化学聚合的过程不同于 ANI, 而且由 NPD

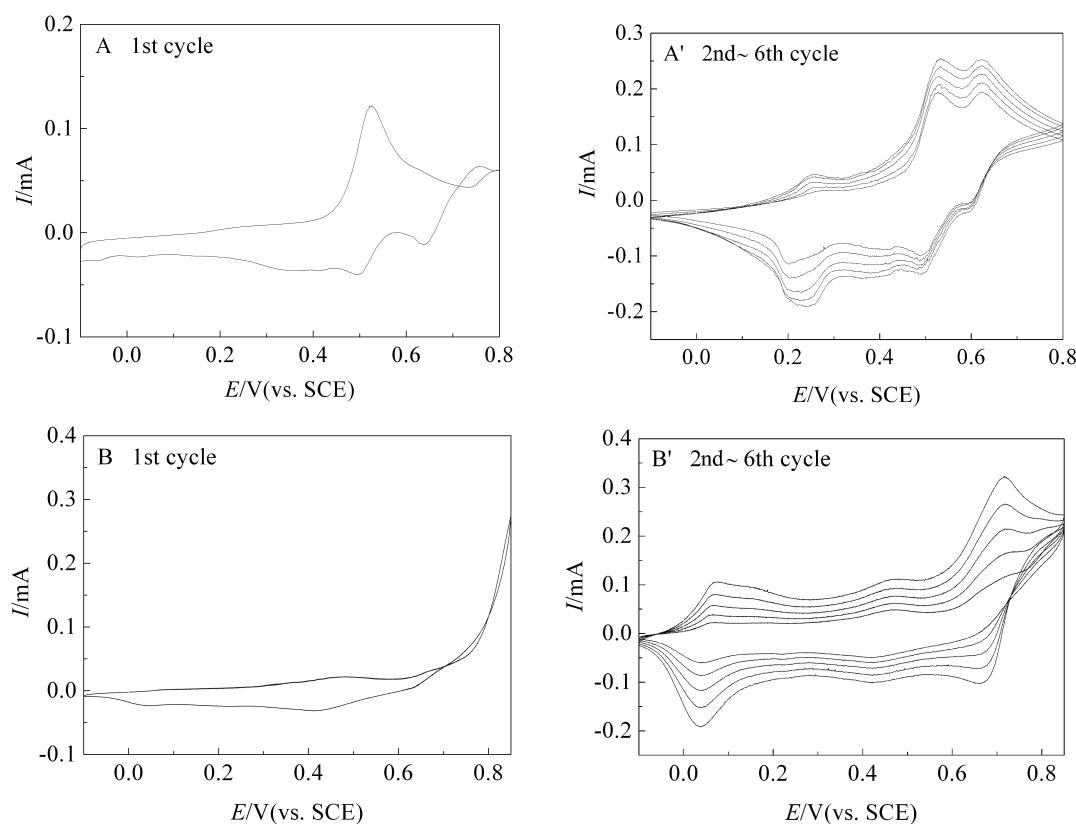


图 1 NPD(A、A')和 ANI(B、B')聚合的循环伏安曲线

Fig. 1 Cyclic voltammograms of GC electrode in  $1\ \text{mol}\cdot\text{L}^{-1}$   $\text{HClO}_4$  solution (20% acetonitrile, by volume) containing  $10\ \text{mmol}\cdot\text{L}^{-1}$  NPD recorded at the 1st cycle (A) and 2nd ~ 6th cycles (A') or  $10\ \text{mmol}\cdot\text{L}^{-1}$  ANI recorded at 1st cycle (B) and 2nd ~ 6th cycles (B') Scan rate:  $50\ \text{mV}\cdot\text{s}^{-1}$

聚合而成的聚合物也有着独特的电化学活性单元结构和性质.

为进一步了解聚合过程,采用恒电流方法考察发生聚合的电位.图2分别是恒电流聚合 NPD(A) 和 ANI(B) 时聚合电位随时间变化( $E-t$ )曲线.从图2可见,在整个聚合过程中,NPD 的聚合电位持续地增加,但增幅仅从 0.45 V 增至 0.49 V;ANI 的聚合电位在 20 s 内从起始的 0.60 V 急剧增至 0.72 V,随后逐渐降到 0.67 V.这些现象表明:NPD 的聚

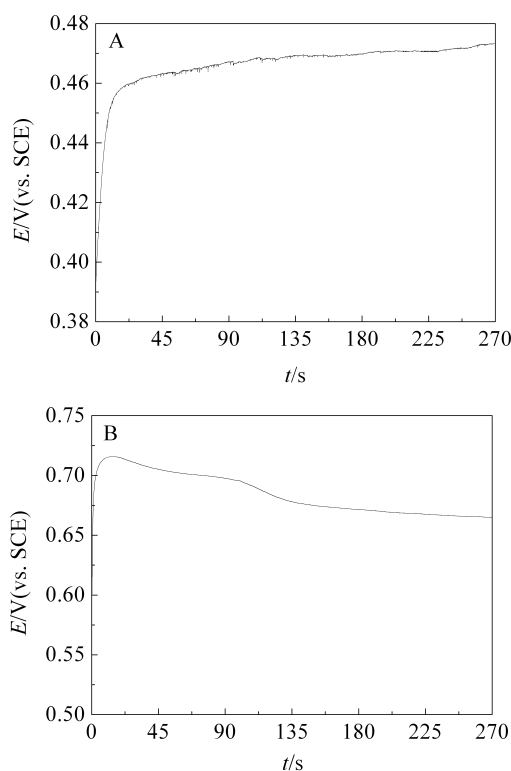


图2 NPD(A)和 ANI(B)恒电流电聚合的  $E-t$  曲线

Fig. 2 Potential-time curves recorded at the steady current of 16  $\mu\text{A}$  for NPD (A) and 10  $\mu\text{A}$  for ANI (B)

Other conditions were the same as those used in Fig. 1

合电位明显低于 ANI 的聚合电位,图 1A' 中位于 0.53 V 的氧化峰为 NPD 的聚合,而图 1B' 中位于 0.70 V 的氧化峰为 ANI 的聚合.由二聚体发生电聚合通常可使聚合物具有好的结构均一性和电学性质<sup>[5,23]</sup>.因此,由 NPD 制备的聚苯胺性能优于由 ANI 单体制备的.

图3是采用恒电流方法分别以 NPD(A)和 ANI(B)为起始单体在 GC 电极表面制备的聚苯胺的 SEM 形貌照片.从图3可见,由 NPD 聚合而成的聚合物为片状结构,大都平行地覆盖在电极表面,而从 ANI 聚合成的聚苯胺由粒径约 30 nm 的颗粒在电极表面构成致密的膜,并且膜顶层可见少量带支链的纤维状结构.这说明单体结构的差异可直接影响聚合物的形貌.

## 2.2 不同 N-苯基对苯二胺单体浓度的聚合物形貌

通过采用大电流密度在电极表面成核、随之小电流密度控制聚合物生长,可由苯胺单体制备得聚

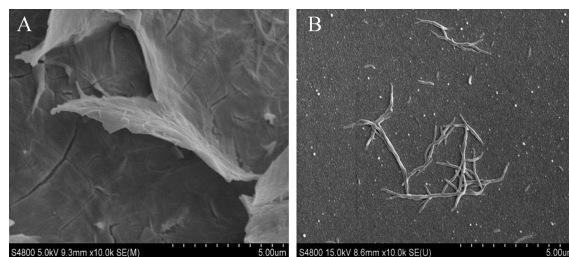


图3 采用恒电流方法分别以 NPD(A)和 ANI(B)为起始单体在 GC 电极表面制备的聚苯胺的 SEM 形貌照片

Fig. 3 SEM images of polyaniline polymerized from NPD (A) and ANI (B) Galvanostatic procedures were according to those shown in Fig. 2, other conditions were the same as those used in Fig. 1

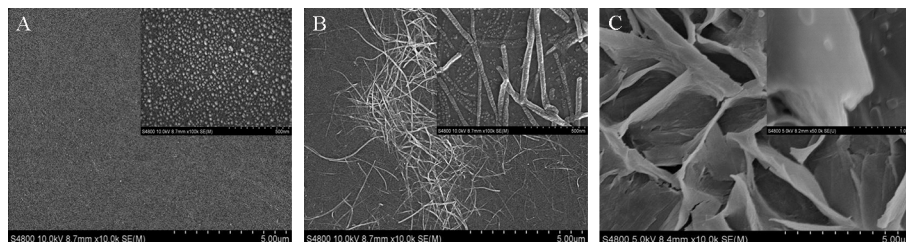


图4 采用分步恒电流在 GC 电极表面制备的聚苯胺 SEM 照片(插图为高放大倍率图)

Fig. 4 SEM images of PANI generated by step-wise galvanostatic method on GC electrodes

Concentrations of NPD monomer: A. 1 mmol·L<sup>-1</sup>; B. 5 mmol·L<sup>-1</sup>; C. 10 mmol·L<sup>-1</sup>

Other conditions were the same as those used in Fig. 1

苯胺纳米线有序阵列<sup>[15-16]</sup>。因此,实验采用分步恒电流法电化学聚合 NPD,探索单体浓度对聚合物形貌的影响,如图 4 所示。从图 4 可见,NPD 单体浓度  $1 \text{ mmol} \cdot \text{L}^{-1}$  时,聚合物以粒径约  $30 \text{ nm}$  的纳米颗粒均匀分散在电极表面(图 4A);当单体浓度提高至  $5 \text{ mmol} \cdot \text{L}^{-1}$ ,纳米颗粒逐渐连接于一起形成直径  $50 \text{ nm}$ 、长度大于  $5 \mu\text{m}$  的聚苯胺超长纳米线(图 4B),并且没有分枝结构;单体浓度进一步提高到  $10 \text{ mmol} \cdot \text{L}^{-1}$ ,聚合物在电极表面形成片状纳米片(长  $4 \mu\text{m}$ ,高  $2 \mu\text{m}$ ,厚  $30 \text{ nm}$ ),并且片与片之间有一定的交联(图 4C)。这些 NPD 单体浓度对聚合物形貌的影响规律与文献报道的采用苯胺单体情形不同,这可能归因于 NPD 分子有更大的  $\pi$  电子共轭体系,在  $\pi$ - $\pi$  共轭和氢键的共同作用下更有利于片状结构的形成,而 ANI 的聚合趋向于构建直线链式结构<sup>[35-37]</sup>。

### 3 结 论

与 ANI 相比,NPD 作电化学制备聚苯胺的起始单体,聚合不仅可较低的电位下进行,而且更易调控聚苯胺形貌结构;当 NPD 单体浓度分别为  $1$ 、 $5$  或  $10 \text{ mmol} \cdot \text{L}^{-1}$  时,采用分步恒电流法能够分别制备出形貌均一的聚苯胺纳米粒子(粒径约  $30 \text{ nm}$ )、超长的纳米线( $> 5 \mu\text{m}$ ,直径  $50 \text{ nm}$ )或大面积纳米片(约长  $4 \mu\text{m}$ ,高  $2 \mu\text{m}$ ,厚  $30 \text{ nm}$ )。

### 参考文献(References):

- [1] Huang J, Virji S, B Weiller H, et al. Polyaniline nanofibers: Facile synthesis and chemical sensors[J]. *Journal of the American Chemical Society*, 2003, 125(2): 314-315.
- [2] Wang Y, Jing X. Intrinsically conducting polymers for electromagnetic interference shielding[J]. *Polymers for Advanced Technologies*, 2005, 16(4): 344-351.
- [3] Rohwerder M, Michalik A. Conducting polymers for corrosion protection: What makes the difference between failure and success[J]. *Electrochimica Acta*, 2007, 53(3): 1300-1313.
- [4] Deshpande M V, Amalnerkar D P. Biosensors prepared from electrochemically-synthesized conducting polymers[J]. *Progress in Polymer Science*, 1993, 18(4): 623-649.
- [5] Stejskal J, Sapurina I, Miroslava Trchová M. Polyaniline nanostructures and the role of aniline oligomers in their formation[J]. *Progress in Polymer Science*, 2010, 35(12): 1420-1481.
- [6] Wang Z Y, Liu S, Wu P, et al. Detection of glucose based on direct electron transfer reaction of glucose oxidase immobilized on highly ordered polyaniline nanotubes[J]. *Analytical Chemistry*, 2009, 81(4): 1638-1645.
- [7] Zhang L J, Zujovic Z D, Peng H, et al. Structural characteristics of polyaniline nanotubes synthesized from different buffer solutions[J]. *Macromolecules*, 2008, 41(22): 8877-8884.
- [8] Zhou C Q, Han J, Song G P, et al. Polyaniline hierarchical structures synthesized in aqueous solution: Micromats of nanofibres[J]. *Macromolecules* 2007, 40(20): 7075-7078.
- [9] Zhang H B, Wang J X, Wang Z, et al. Electrodeposition of polyaniline nanostructures: A lamellar structure[J]. *Synthetic Metals*, 2009, 159(3/4): 277-81.
- [10] Li Y, Wang B C, Feng W. Chiral polyaniline with flaky, spherical and urchin-like morphologies synthesized in the L-phenylalanine saturated solutions[J]. *Synthetic Metals*, 2009, 159(15/16): 1597-602.
- [11] Zujovic Z D, Laslau C, Travas-Sejdic J. Lamellar-structured nanoflakes Comprised of stacked oligoaniline nanosheets[J]. *Chemistry-An Asian Journal*, 2011, 6(3): 791-796.
- [12] Huczko A. Template-based synthesis of nanomaterials[J]. *Applied Physics A-Materials Science & Processing*, 2000, 70(4): 365-376.
- [13] Gao M, Huang S, Dai L, et al. Aligned coaxial nanowires of carbon nanotubes sheathed with conducting polymers[J]. *Angewandte Chemie International Edition*, 2000, 39(20): 3664-3667.
- [14] Wan M. A template-free method towards conducting polymer nanostructures[J]. *Advanced Materials*, 2008, 20(15): 2926-2932.
- [15] Liang L, Liu J, Windisch C F, et al. Direct assembly of large arrays of oriented conducting polymer nanowires[J]. *Angewandte Chemie International Edition*, 2002, 41(19): 3665-3668.
- [16] Gao Y X (高艳新), Sun L C (孙丽超), Xie S Y (谢素原), et al. Electrochemical fabrication of the ordered polyaniline nanowires array[J]. *Journal of Electrochemistry (电化学)*, 2012, 18(1): 51-55.
- [17] Liu J, Lin Y, Liang L, et al. Templateless assembly of molecularly aligned conductive polymer nanowires: A new approach for oriented nanostructures[J]. *Chemistry-A European Journal*, 2003, 9(3): 605-611.
- [18] Wu L L (吴玲玲), Luo J (罗谨), Lin Z H (林仲华). Spec-

- Chinese Universities (高等学校化学学报), 1997, 18(10): 1657-1663.
- [19] Wu L L, Luo J, Lin Z H. Spectroelectrochemical studies of poly-o-phenylenediamine. Part 1. *In situ* resonance raman spectroscopy [J]. Journal of Electroanalytical Chemistry, 1996, 417(1): 53-68.
- [20] Randriamahazaka H, Sini G, Tran Van F. Electrodeposition mechanisms and electrochemical behavior of Poly (3,4-ethylenedithiathiophene) [J]. Journal of Physical Chemistry C, 2007, 111(12): 4553-4560.
- [21] Si S H, Xu Y J, Nie L H, et al. Electrochemical quartz crystal microbalance study on electropolymerization of m-phenylenediamine: Effects of aniline and polyaniline [J]. Electrochimica Acta, 1995, 40(17): 2715-2721.
- [22] Li X, Huang M, Duan W. Novel multifunctional polymers from aromatic diamines by oxidative polymerizations[J]. Chemical Reviews, 2002, 102(9): 2925-3030.
- [23] Heinze J, Frontana-Urbe B A, Ludwigs S. Electrochemistry of conducting polymers-persistent models and new concepts [J]. Chemical Reviews, 2010, 110(8): 4724-4771.
- [24] Heinze J, Rasche A, Pagels M, et al. On the origin of the so-called nucleation loop during electropolymerization of conducting polymers[J]. Journal of Physical Chemistry B, 2007, 111(5): 989-997.
- [25] Lindoy L F, Atkinson I M, Editors. Self-assembly in supramolecular systems[M]. Royal Society of Chemistry, Cambridge, 2000.

## Preliminary Study on Morphology Controllability of Electrochemically Prepared Polyaniline by Using Aniline Aimer

ZUO Yang, SHI Kang\*

(College of Chemistry and Chemical Engineering, Xiamen University, Xiamen 361005, Fujian, China)

**Abstract:** Employing of aniline dimer (N-phenyl-p-phenylenediamine, NPD) as the starting monomer, polyaniline was electrochemically synthesized on the surface of glassy carbon electrode in acetonitrile-aqueous mixing solutions (20%, by volume) containing  $1 \text{ mol} \cdot \text{L}^{-1} \text{ HClO}_4$ . Experimental results demonstrated that the polymerization of NPD occurs at the potentials about 0.2 V lower than those of aniline monomer. Furthermore, the resulting polyaniline has higher morphology controllability than those synthesized by using aniline as the stating monomer. The uniform polyaniline nanoparticles (30 nm in diameter), ultralong nanowires (length > 5  $\mu\text{m}$ , 50 nm in diameter) or large area nanosheets (4  $\mu\text{m}$  in length, 2  $\mu\text{m}$  in height, 30 nm in thickness) can be prepared by using step-wise galvanostatic method when the concentrations of NPD monomer was 1, 5 or 10  $\text{mmol} \cdot \text{L}^{-1}$ , respectively.

**Key words:**  $\pi$ -conjugated type of organic conducting polymer; polyaniline; monomer; electrochemical polymerization; uniform morphology